13th World Conference on Earthquake Engineering
Vancouver, B.C., Canada
August 1-6, 2004
Paper No. 1853

EFFECTS OF THE VERTICAL GROUND MOTIONS ON THE NON-LINEAR ANALYSIS OF REINFORCED CONCRETE FRAMES

Tiziano PEREA [1] and Luis ESTEVA [2]

SUMMARY

The influence of the vertical seismic component on the non-linear dynamic response of some reinforced concrete structures is studied. Subject structures are analyzed and designed according to current seismic design practices, estimating the lateral forces from modal spectral analysis, neglecting in this phase of the design the effect of the vibration in the vertical direction. Then, nonlinear dynamic analyses of representative frames with elastic-perfectly-plastic behavior are conducted using Drain-2DX software, considering the horizontal component with and without the incorporation of the corresponding vertical component. Dynamic responses obtained for the horizontal component acting alone are compared with those obtained from the simultaneous application of both seismic components. The influence of the frequencies of the vertical vibration modes is discussed in the paper, as well as the response trends related to the possibility of occurrence of significant dynamic response in the vertical direction. Based upon the described study, some qualitative recommendations are provided to include the influence of the vertical seismic component for the structural design of reinforced concrete structures.

INTRODUCTION

The analytical studies based on the effects of the vertical component of the seismic ground motion on the structural behavior have consisted in investigating elastic and inelastic dynamic responses of different structural systems subject to the action of the vertical seismic component, combining them with the effects of the horizontal component and gravity loads. Most of the analytical studies have been focused on studies of reinforced concrete and steel bridges and frames. Some studies have been related to field observations (Papazoglou and Elnashai [1]; Elnashai [2]), and very few of them have been related to experimental studies (Tani and Soda [3]). A state-of-the-art about analytical studies of the vertical ground motion and its influence on the structural response was drafted by Perea [4].

[1] Universidad Autónoma Metropolitana (UAM-A), Mexico, E-mail: tperea@correo.azc.uam.mx
[2] Instituto de Ingeniería - UNAM, Mexico, E-mail: LEstevaM@iingen.unam.mx

REINFORCED CONCRETE BEAMS

Vertical vibration periods

General equations to calculate vertical vibration periods (T_{VN}) of beams with distributed mass and their corresponding modal forms (ϕ), which are derived from the classical beam vibration theory, have been reported by Young-Budynas [5] and Chopra [6] based on the results of Huang [7].

$$T_{VN} = \frac{2\pi}{K_N}\sqrt{\frac{w \cdot L^4}{g \cdot EI}} \tag{1}$$

$$\phi(x) = C_1 \mathrm{sen}\beta x + C_2 \cos\beta x + C_3 \mathrm{senh}\beta x + C_4 \cosh\beta x \tag{2}$$

Where T_{VN} is the vertical period corresponding to the N mode of vibration. $\phi(x)$ is the function that defines the N modal form at point x of the beam ($0<x<L$). w, L and EI are the uniform load, the span-length, and the elastic stiffness in bending, respectively. g is the acceleration of gravity. C1, C2, C3 and C4 are constants that depend on the beam restraints. The square of the characteristic parameter β is equal to:

$$\beta^2 = \frac{2\pi}{T}\sqrt{\frac{w \cdot L}{g \cdot EI}} \tag{3}$$

In Table 1, the values K_N calculated by Huang [7] are presented in order to evaluate, with different restraint conditions (DF: fixed at both ends, SS: simply-supported, CB: cantilevers), the first five periods of vertical beam vibration. These values, K_N, are results of substituting the limit conditions in the expression that is derived from the classical beam vibration theory (Equation 1).

Table 1. K_N Constant for five vertical modes of vibration of beams with uniform load and different restraint conditions (DF: fixed at both ends, SS: simply-supported, CB: cantilevers).

Mode	K_N	DF	SS	CB
1	K_1	22.4	9.87	3.516
2	K_2	61.7	39.48	22.03
3	K_3	121	88.83	61.70
4	K_4	200	157.91	120.90
5	K_5	299	246.74	199.86

In case of simply-supported beams (SS) with uniform load (w), the exact solution to calculate the vertical periods of vibration and the corresponding modal forms (Chopra [6]) is:

$$T_{VN} = \frac{2\pi}{(N\pi)^2}\sqrt{\frac{wL^4}{g \cdot EI}} \tag{4}$$

$$\phi(x) = \mathrm{sen}\frac{N\pi x}{L} \tag{5}$$

The fundamental vertical period can also be estimated with quite accurately with a discrete mass model according to the Rayleigh quotient (Chopra [6]):

$$T = 2\pi\sqrt{\frac{\sum_{i=1}^{n} m_i u_i^{\,2}}{g\sum_{i=1}^{n} m_i u_i}} \approx \frac{2\pi}{1.2}\sqrt{\frac{u_{max}}{g}} \tag{6}$$

Where m_i and u_i are the discreet mass and the vertical displacement of the i-th discrete point, respectively. u_{max} is the maximum vertical displacement.

Dynamic step-by-step analysis of beams

Reinforced concrete beams with discrete mass, ξ=5% of critical damping, and three common support conditions are modeled: fixed at both ends (DF), simply-supported (SS), and cantilever (CB). The beams were designed to resist their self-weight and a uniform load of 4T/m, determining the beam-span in order to have in all cases a fundamental vertical period equal to 0.1s.

In Table 2, the periods (Tv) associated with the vertical modes of vibration obtained with the Drain-2DX software (Prakash et al. [8]; Powell [9]), their corresponding participation factors (Γ), and percentages of effective mass (m^*) are shown.

Table 2. Modal analysis results

	Fixed at both ends (DF)			Simply-supported (SS)			Cantilever (CB)		
Mode	T_v	Γ	m^*	T_v	Γ	m^*	T_v	Γ	m^*
1	0.100	1.63	0.67	0.100	1.34	0.70	0.100	0.85	0.49
2	0.025	0.70	0.12	0.018	0.30	0.04	0.025	0.56	0.22
3	0.014	0.48	0.06	0.009	0.12	0.01	0.012	0.34	0.08
4	0.010	0.46	0.05	0.008	0.61	0.15	0.009	0.35	0.08
$\sum$			0.90			0.89			0.87

Dynamic step-by-step analyses of beams with common support conditions, and using vertical ground motion records, were made. In Table 3, the values of the maximum plastic hinge rotations are shown. In these analyses, where the vertical resonant effect was studied, the following trends were observed:

- In beams fixed at both ends (DF), similar plastic hinge rotations are presented at mid-span (DFc) and at the ends (DFe) of the element due to increments in negative and positive moments, respectively. In order to provide greater ductility capacity to withstand the increasing flexural demand, it will be necessary to provide a sufficient amount of transverse reinforcement and/or compression steel, even for the mid-span section, where it is common practice to use greater separation of ties and minimum compression reinforcement with respect to the beam-ends.

- In simply-supported beams (SS), rotations are presented only at mid-span (SSc) due to increments in the positive moment. In order to provide greater ductility capacity to withstand the increasing flexural demand, it will be necessary to provide a sufficient amount of transverse reinforcement and/or compression steel, this is, a greater amount than the one that is commonly used for this type of beams under the action of gravitational loading alone.

- In cantilever beams (CB), the plastic hinge rotation is presented in the fixed end (CBe) by an increment of the negative flexural demand. In order to provide greater ductility capacity at the fixed end, it will be necessary to provide a sufficient amount of transverse reinforcement and/or compression steel.

For beams with the discussed common support conditions that have the same period and spectral demands in acceleration and displacement, similar rotation values were obtained. The latter indicates that the expected damage level for these beams is function of the earthquake intensity associated with the vertical period. This fact contradicts some recommended provisions because, according to them, just some elements (i.e. cantilever, prestressed and/or long-span beams), are vulnerable to vertical ground motions.

Peak plastic hinge rotations in beams with simple support conditions were obtained with the most intense records, i.e., those having the greater displacement and spectral pseudo-acceleration (Sa>1.6g) corresponding to the fundamental vertical period (Tv=0.1s). These records correspond to stations with the nearest epicentral distance and focal depth from the source (records of the Mexicali Valley).

Table 3. Plastic hinge rotations obtained from analysis with vertical ground motion records (T_v=0.1s)

RECORDS	M	D (km)	SOIL & SITE	Sd (cm)	Sa (g)	DFe R1	DFc R2	SSc R3	CBe R4
VICS800609	6.1	15	Sediments, Mexicali, Baja California	1.09	4.30	0.075	0.066	0.082	0.075
VCPS870207	5.4	8	Rock, Mexicali, Baja California	0.42	1.66	0.017	0.016	0.022	0.017
IAGS791015	6.6	10	Sediment, Mexicali, Baja California	0.13	0.50	0.008	0.007	0.004	0.009
ZACA850919	8.1	86	Clay, Zacatula, Michoacán	0.13	0.51	0.003	0.003	0.005	0.002
CALE970111	6.9	40	Rock, Caleta de Campos, Michoacán	0.12	0.46	0.002	0.002	0.003	0.001
RIXC951021	6.5	112	Limestone, Tuxtla Gutiérrez, Chiapas	0.10	0.33	0.000	0.000	0.000	0.000
BALC941210	6.3	43	Rock, El Balcón, Guerrero	0.08	0.31	0.000	0.000	0.000	0.000
COPL931025	6.6	20	Rock, Copala, Guerrero	0.06	0.25	0.000	0.000	0.000	0.000
CALE850919	8.1	25	Rock, Caleta de Campos, Michoacán	0.05	0.22	0.000	0.000	0.000	0.000

Record names (EEEEYYMMDD) mean station name (EEEE), last two digits of year (YY), month (MM) and day (DD) of the earthquake. M: Magnitude. D: Hipocentral distance (km). Sd & Sa are the spectral displacement and the spectral pseudo-acceleration associated with the fundamental vertical period (Tv=0.1s). R1, R2, R3 and R4 are the maximums plastic hinge rotations in fixed ends (DFe, CBe) and in the mid-span (DFc & SSc).

It is important to indicate that, for analysis and design of these beams, the contribution of the slab to the increment of their resistance and stiffness was neglected. If it had been considered, the vertical seismic component effects would tend to be affected; the study of this last point would be of interest for a future research.

Vertical vibration periods

An expression for the estimation of the vertical period for beams with common support conditions was previously presented, as a function of the elastic stiffness in bending, the uniform load, the beam-span, and the non-dimensional parameter of the restraint condition (Huang [7]). This expression is summarized as:

$$T_{VN} = \frac{2\pi}{K_N}\sqrt{\frac{w \cdot L^4}{g \cdot EI}} \tag{7}$$

Where T_V it is the vertical period. K_N is the non-dimensional parameter that depends on the restraint conditions. w is the uniform distributed load. L is the beam-span. g is the gravity constant. EI is the stiffness of the beam in bending.

As it was previously presented, the value of the non-dimensional constant K_1 associated with fundamental vertical period tends, according to Huang [7], to a value of 9.87 for the double-hinged restraints (SS) and 22.40 for the double-fixed restraints (DF). As it is known, actually neither perfectly fixed nor perfectly hinged joints are produced. Therefore, in the case of frame beams an intermediate restraint condition among the previous cases would be adequate ($9.81<K_1<22.40$).

For eight cases where the vertical period and the EI beam to column ratio are known, the constants K_1 were calculated. A curve is fitted to the results (Figure 1, Equation 8), which has a high determination coefficient ($r^2 = 0.8$) and is consistent with both limit conditions.

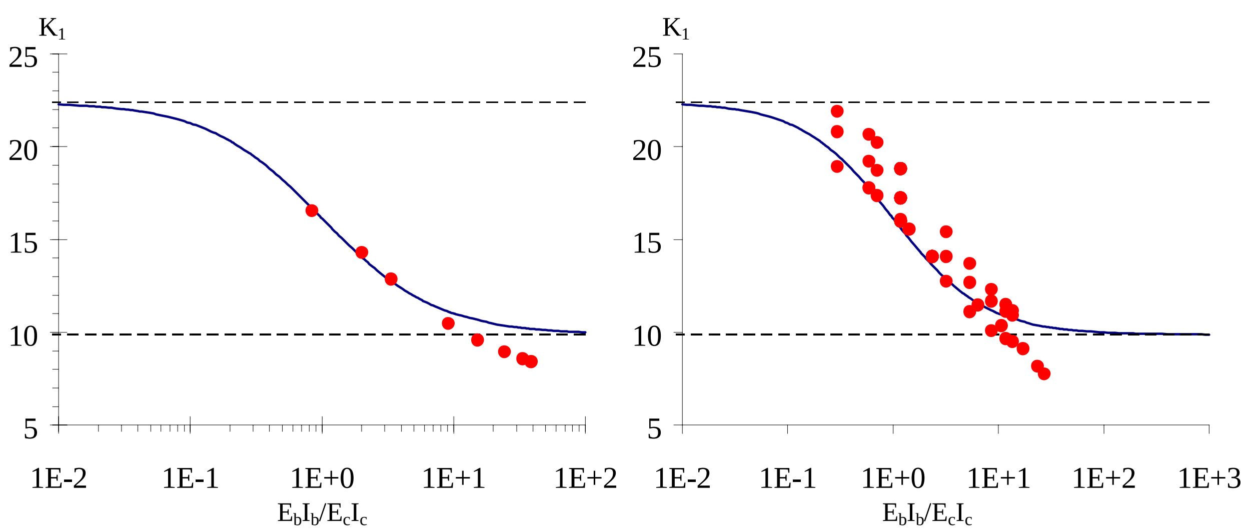

a) Generated from the data b) Compared with other results

Figure 1. Comparison of K_1 constants and the fitted curve

Substituting constant K_1 in equation 7, it is possible to estimate the vertical periods of beams associated with frames, and without the necessity of considering a model with distributed mass.

$$K_1 = \frac{\pi^2 (E_b I_b / E_c I_c) + 22.4}{E_b I_b / E_c I_c + 1} \quad (8)$$

$$T_{V1} = \frac{2\pi(E_b I_b / E_c I_c + 1)}{\pi^2 (E_b I_b / E_c I_c) + 22.4} \sqrt{\frac{w \cdot L^4}{g \cdot E_b I_b}} \quad (9)$$

Subsequent studies could be aimed at monitoring the proposed equation with other models, or to optimize it with a more data regression, or incorporating other variables. In this way, Sovero [10] obtained an expression to calculate the fundamental vertical period of some frames with fixed and hinged restraints (Equation 10).

$$T_{V1} = \sqrt{\frac{\pi^2 \cdot w \cdot L^4}{3072 \cdot g \cdot EI} \left[\frac{128B + 13m + \sqrt{15488B^2 + 2816Bm + 137m^2}}{(2B + m)} \right]} \quad (10)$$

$$B = \frac{I_b \cdot H}{I_c \cdot L} \quad (11)$$

In the last formulas, B is function of the beam (I_b) and column (I_c) inertia moments, the story height (H), and the span-length (L). The coefficient m depends on the restraint conditions: m=3 for hinged restraints, and m=4 for fixed restraints.

As it was previously commented, the fundamental vertical period can also be estimated quite accurately and easily with a discrete mass model according to the Rayleigh quotient (Chopra [6]). In this equation, m_i is the discrete mass, and u_i is the displacement under the action of gravitational loads at the i-th discrete point. u_{max} is the maximum vertical displacement.

$$T = 2\pi \sqrt{\frac{\sum_{i=1}^{n} m_i u_i^2}{g \sum_{i=1}^{n} m_i u_i}} \approx \frac{2\pi}{1.2} \sqrt{\frac{u_{max}}{g}} \quad (12)$$

Dynamic step-by-step analysis of moment resistant frames

The influence of the vertical seismic component on some reinforced concrete frames, with elastic-perfectly-plastic behavior and different geometric properties, is studied. All of them are shown in Figure 2: one story - one bay (1S1B), four stories - one bay (4S1B), four stories - two bays (4S2B), ten stories - one bay (10S1B). The structures are designed according to the current design practices neglecting the vertical seismic component. Then, the structures are modeled in Drain-2DX considering discrete mass points spaced at one tenth of the beam-span, and ξ=5% critical damping for both horizontal and vertical fundamental modes. Finally, their non-linear dynamic behavior is studied based on step-by-step dynamic analysis for a set of ground motion records associated with earthquakes originated in the subduction zone of the Mexican Pacific Coast.

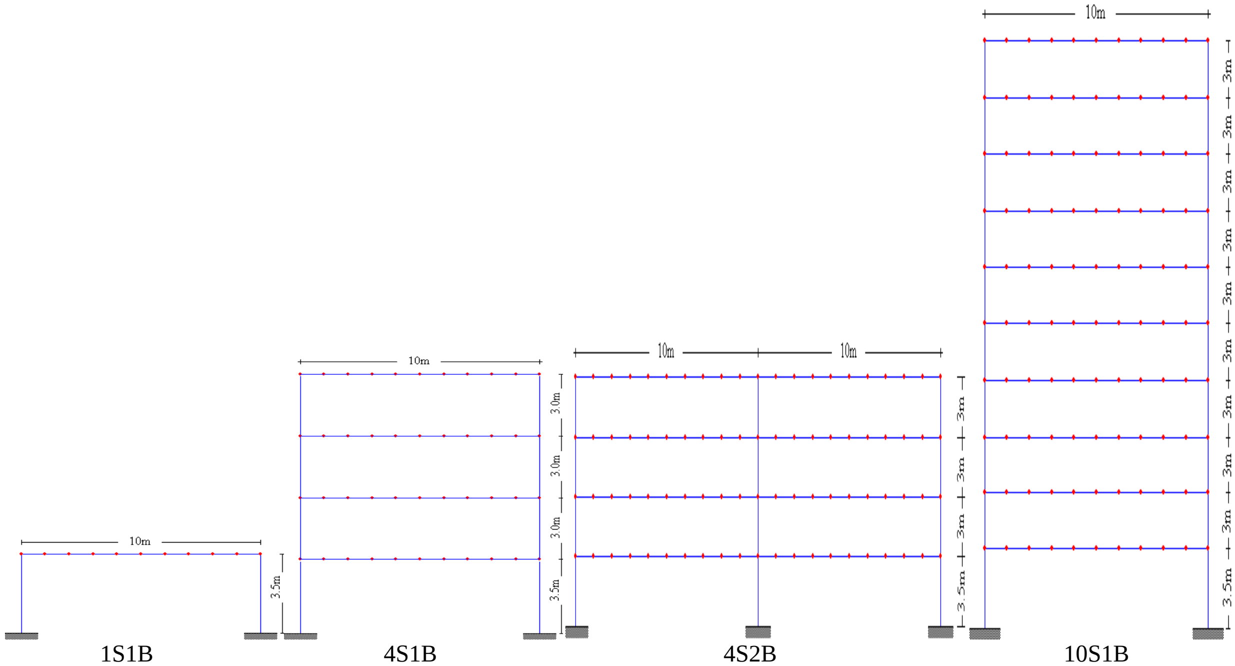

Figure 2. Reinforced concrete moment resistant frames

The acceleration stories considered in the dynamic analysis are listed in Table 4. The record names (EEEEYYMMDD) mean station name (EEEE), last two digits of year (YY), month (MM) and day (DD) of the earthquake.

Table 4. Information of the records selected for the step-by-step analysis

RECORD	M	R	H	D	SOIL	SITE
VCPS870207	5.4	6	6	8	Volcanic rocks	Mexicali Valley, Baja California
IAGS791015	6.6	3	10	10	Sediments (alluvium)	Mexicali Valley, Baja California
VICS800609	6.1	10	12	15	Sediments (alluvium)	Mexicali Valley, Baja California
COPL931025	6.6	7	19	20	Rock	Copala, Guerrero
CALE850919	8.1	21	15	25	Rock	Caleta de Campos, Michoacán
CALE970111	6.9	30	16	40	Rock	Caleta de Campos, Michoacán
BALC941210	6.3	38	20	43	Rock	El Balcón, Guerrero
ACAC890425	6.9	56	15	58	Sand, lime, clay	Acapulco, Guerrero
ZACA850919	8.1	84	15	86	Compact clay	Zacatula, Michoacán
RIXC951021	6.5	54	98	112	Limestone	Tuxtla Gutiérrez, Chiapas

M: Magnitude; R: Epicentral distance (km); H: Focal depth (km); D: Hypocentral distance (km).

Based on both Mexican ground motion records and dynamic step-by-step analyses for the structures under study, the following observations can be done:

A. If the system remains elastic under the action of gravitational loads and the vertical seismic component, both global and local responses are practically identical when: (1) the horizontal component acts alone and (2) when the horizontal and vertical components act simultaneously.

B. If the system reaches the non-linear behavior under the action of gravitational loads and the vertical seismic component, both global and local responses are notably different when (1) the horizontal component acts alone and (2) when the horizontal and vertical components act simultaneously.

The second case (case B), where the vertical component influenced both global and local responses of frames, was result of the step-by-step analysis with records VICS800609 and VCPS870207 (Figure 3.ii, Figure 4.ii, Figure 5.ii, Figure 6, Figure 7 and Figure 8). With these records, spectral pseudo-accelerations were greater than 1.8g (Table 5, Table 7, Table 9 and Table 10). They produced plastic hinge rotations at the mid-span and at the ends of some beams, and at the ends of some columns, with the values listed in Table 6 for model 1S1B, and in Table 8 for model 4S1B.

With the vertical component of the rest of the records, which have spectral pseudo-accelerations smaller than 0.40g, the behavior of the frames turned out to be elastic (case A), and therefore, the global and local responses of frames, including and excluding vertical component are practically identical (Figure 3.i, Figure 4.i, Figure 5.i).

Table 5. Spectral intensity demands for frame 1S1B (T_H=0.17s, T_V=0.14s)

		Spectral displacement (cm)			Spectral pseudo-acceleration (g)		
RECORD	CASE	N-S	E-W	V	N-S	E-W	V
VCPS870207	B	1.91	1.68	0.96	2.61	2.30	1.94
VICS800609	B	1.26	1.20	1.02	1.72	1.64	2.05
IAGS791015	A	0.29	0.24	0.16	0.39	0.33	0.29

a) H b) ±V c) H±V

i) Elastic behavior in dynamic analysis with vertical ground motion (case A)

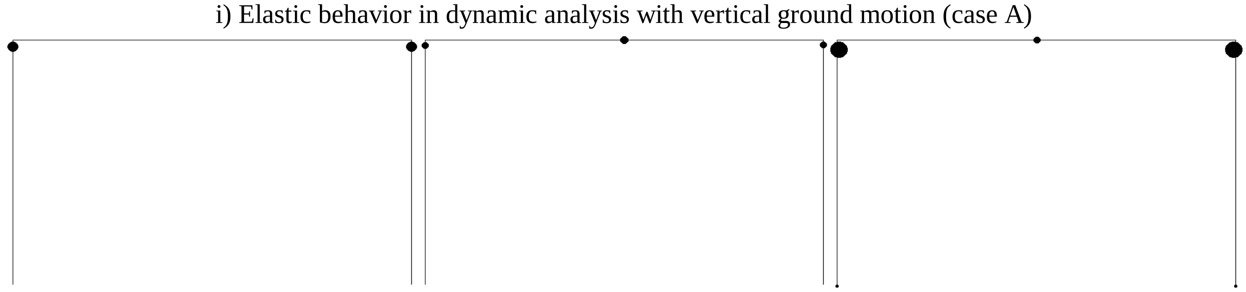

a) H b) ±V c) H±V

ii) Inelastic behavior in dynamic analysis with vertical ground motion (case B)

Figure 3. Distribution of plastic hinge rotations

Table 6. Summary of plastic hinge rotations, both accumulated and maximum, shown in Figure 3.ii

Record VICS800609								
Element \ Case	H_{N-S}	H_{E-W}	+V	-V	H_{N-S}+V	H_{E-W}+V	H_{N-S}-V	H_{E-W}-V
Mid-span	0.0000	0.0000	0.0107	0.0098	0.0183	0.0165	0.0130	0.0124
Superior end of columns	0.0308	0.0258	0.0110	0.0093	0.0526	0.0456	0.0447	0.0417

Record VCPS870207								
Element \ Case	H_{N-S}	H_{E-W}	+V	-V	H_{N-S}+V	H_{E-W}+V	H_{N-S}-V	H_{E-W}-V
Mid-span	0.0000	0.0000	0.0051	0.0052	0.0061	0.0063	0.0066	0.0070
Superior end of columns	0.0039	0.0022	0.0039	0.0037	0.0093	0.0096	0.0121	0.0098

Table 7. Spectral intensity demands for frame 4S1B (T_H=0.51s, T_V=0.15s)

		Spectral displacement (cm)			Spectral pseudo-acceleration (g)		
RECORD	CASE	N-S	E-W	V	N-S	E-W	V
VICS800609	B	4.37	4.98	1.10	0.66	0.76	1.92
VCPS870207	B	4.37	7.29	1.03	0.66	1.11	1.81
IAGS791015	A	3.49	3.96	0.16	0.53	0.60	0.29
ZACA850919	A	4.03	2.91	0.15	0.61	0.44	0.27
BALC941210	A	0.84	0.65	0.12	0.13	0.10	0.21

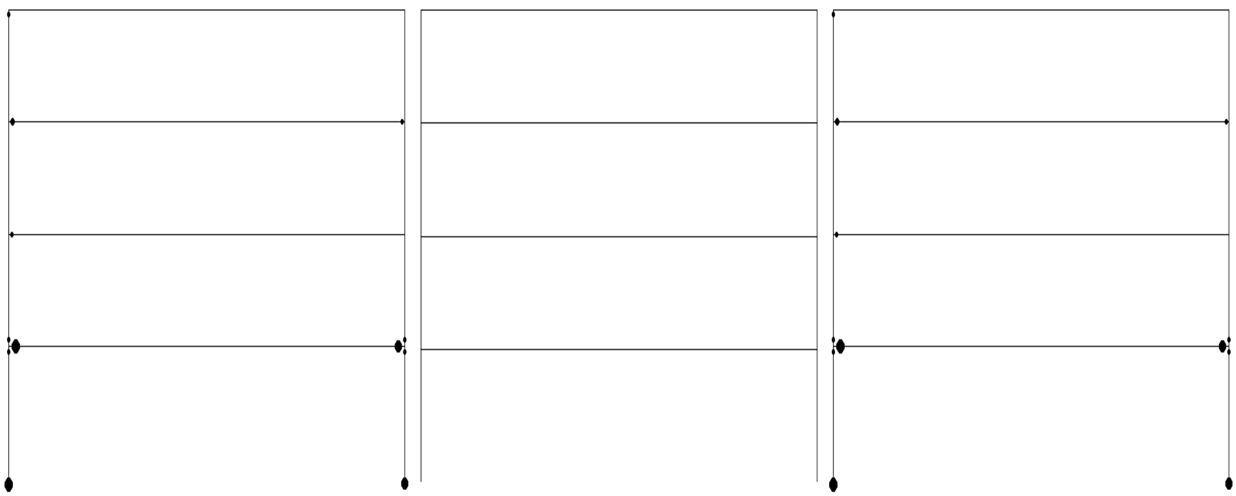

a) H b) ±V c) H±V

i) Elastic behavior in dynamic analysis with vertical ground motion (case A)

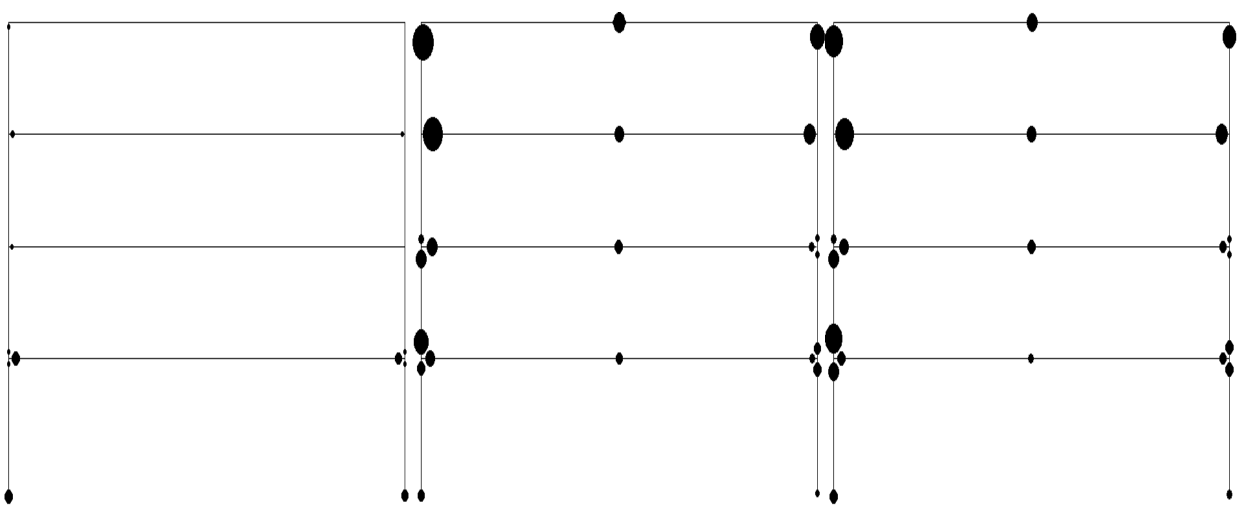

a) H b) ±V c) H±V

ii) Inelastic behavior in dynamic analysis with vertical ground motion (case B)

Figure 4. Distribution of plastic hinge rotations

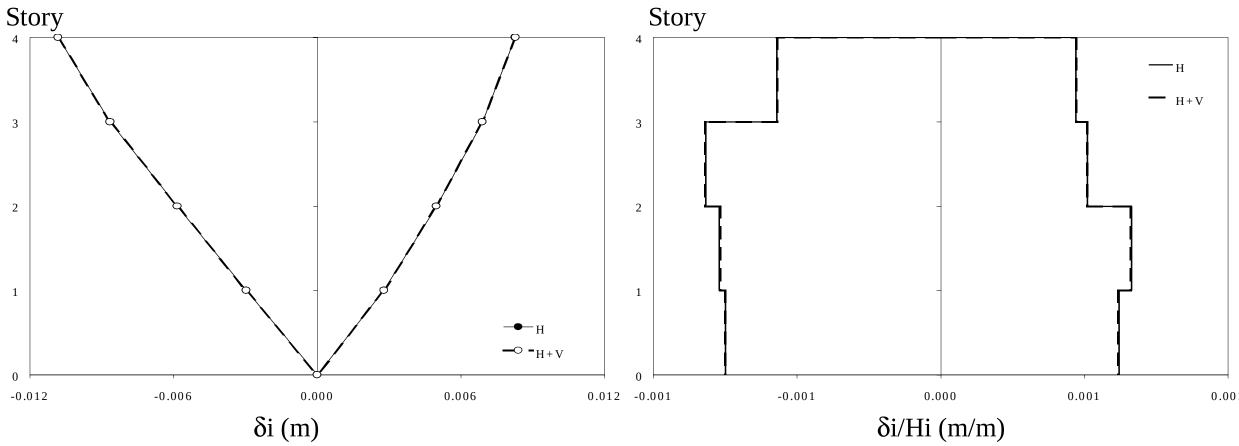

i) Elastic behavior in dynamic analysis with vertical ground motion (case A)

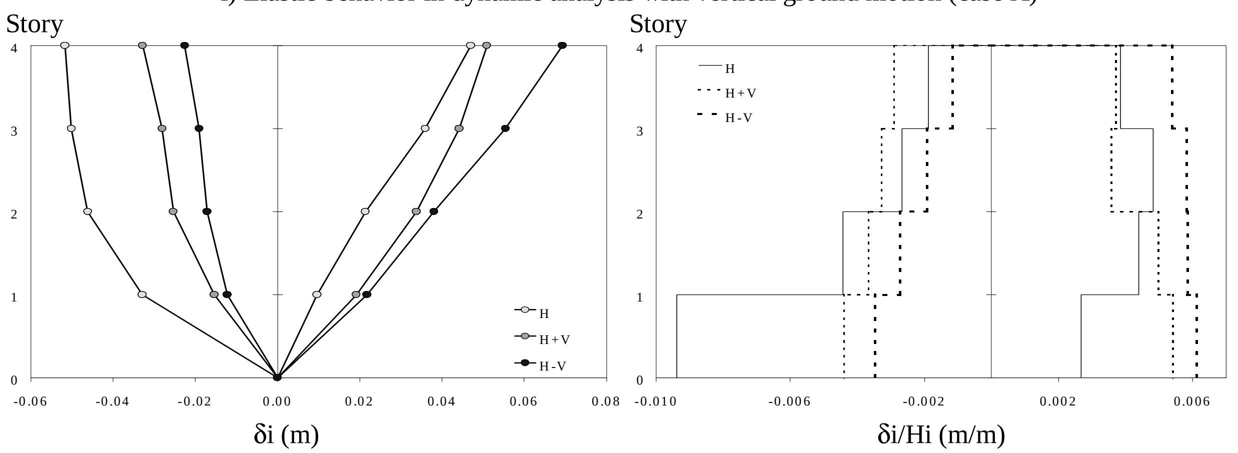

ii) Inelastic behavior in dynamic analysis with vertical ground motion (case B)

Figure 5. Stories displacement and drift

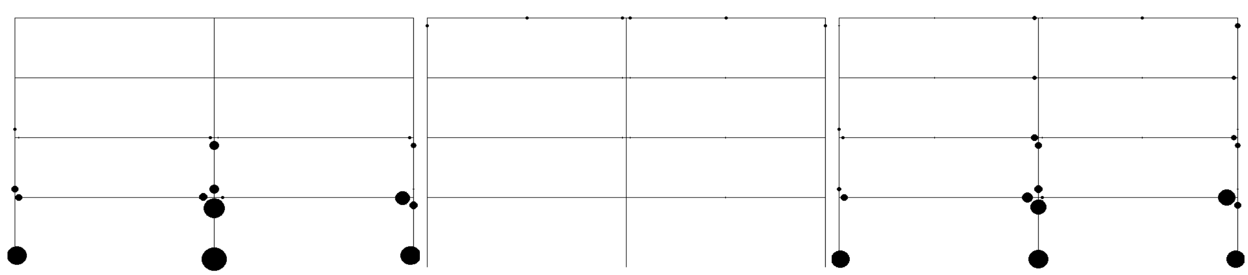

a) H b) ±V c) H±V

i) Inelastic behavior in dynamic analysis with vertical ground motion from VCPS870207 record (case B)

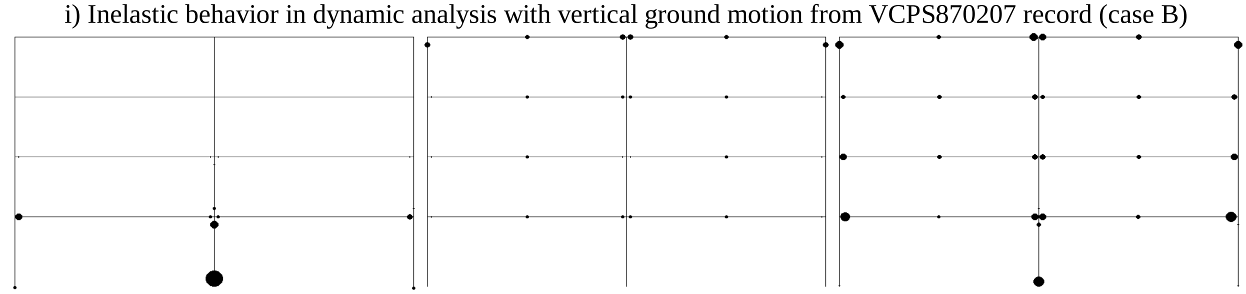

a) H b) ±V c) H±V

ii) Inelastic behavior in dynamic analysis with vertical ground motion from VICS800609 record (case B)

Figure 6. Distribution of plastic hinge rotations in model 4S2B

Table 8. Summary of accumulated and maximum plastic hinge rotations obtained from the analysis of 4S1B frame from VICS800609 record, and shown in the Figure 4.ii

MAXIMUM PLASTIC HINGE ROTATIONS AT BEAM MID-SPAN

Story	$H_{N\text{-}S}$	$H_{E\text{-}W}$	+V	-V	$H_{N\text{-}S}$+V	$H_{N\text{-}S}$-V	$H_{E\text{-}W}$+V	$H_{E\text{-}W}$-V
4	-	-	-0.014	-0.013	-0.017	-0.015	-0.017	-0.014
3	-	-	-0.012	-0.011	-0.014	-0.013	-0.013	-0.012
2	-	-	-0.010	-0.010	-0.012	-0.012	-0.010	-0.010
1	-	-	-0.007	-0.007	-0.009	-0.008	-0.007	-0.007

MAXIMUM PLASTIC HINGE ROTATIONS AT BEAM ENDS

Story	$H_{N\text{-}S}$	$H_{E\text{-}W}$	+V	-V	$H_{N\text{-}S}$+V	$H_{N\text{-}S}$-V	$H_{E\text{-}W}$+V	$H_{E\text{-}W}$-V
4	-	-	-	-	-	-	-	-
3	0.006	0.009	0.013	0.012	0.028	0.026	0.025	0.028
2	0.004	0.004	0.004	0.004	0.016	0.014	0.014	0.017
1	0.012	0.016	-	-	0.014	0.011	0.014	0.013

MAXIMUM PLASTIC HINGE ROTATIONS IN COLUMNS

	POSITIVE					NEGATIVE		
Story	+V	-V	H	H+V	H-V	H	H+V	H-V
4s	0.018	0.015	0.004	0.031	0.028	-0.002	-0.021	-0.020
4i	-	-	-	0.001	-	-	-	-0.001
3s	-	-	-	-	-	-	-	-
3i	0.003	0.004	0.002	0.006	0.005	-	-0.007	-0.008
2s	0.005	0.005	0.002	0.015	0.015	-0.002	-0.005	-0.006
2i	0.007	0.007	0.004	0.009	0.012	-0.005	-0.022	-0.024
1s	0.005	0.005	0.003	0.011	0.016	-0.005	-0.012	-0.012
1i	-	-	0.005	0.005	0.005	-0.005	-0.005	-0.006

ACCUMULATED PLASTIC HINGE ROTATIONS IN COLUMNS

	POSITIVE					NEGATIVE		
Story	+V	-V	H	H+V	H-V	H	H+V	H-V
4s	0.018	0.015	0.004	0.031	0.028	-0.002	-0.021	-0.020
4i	-	-	-	0.001	-	-	-	-0.001
3s	-	-	-	-	-	-	-	-
3i	0.003	0.004	0.002	0.006	0.005	-	-0.007	-0.008
2s	0.005	0.005	0.002	0.015	0.015	-0.002	-0.005	-0.006
2i	0.007	0.007	0.004	0.009	0.012	-0.005	-0.022	-0.024
1s	0.005	0.005	0.003	0.011	0.016	-0.005	-0.012	-0.012
1i	-	-	0.011	0.007	0.008	-0.015	-0.012	-0.014

Table 9. Spectral intensity demands for frame 4S1B (T_H=0.64s, T_V=0.13s)

		Spectral displacement (cm)			Spectral pseudo-acceleration (g)		
RECORD	CASE	N-S	E-W	V	N-S	E-W	V
VICS800609	B	6.56	8.34	0.99	0.63	0.80	2.32
VCPS870207	B	8.08	13.40	0.86	0.78	1.29	2.01
IAGS791015	A	4.50	4.29	0.15	0.43	0.41	0.34

Table 10. Spectral intensity demands for frame 10S1B (T_H=1.0s, T_V=0.12s)

		Spectral displacement (cm)			Spectral pseudo-acceleration (g)		
RECORD	CASE	N-S	E-W	V	N-S	E-W	V
VICS800609	B	10.22	9.19	1.04	0.40	0.36	2.84
VCPS870207	B	10.90	14.52	0.74	0.43	0.57	2.01
IAGS791015	A	6.69	6.79	0.13	0.26	0.27	0.37

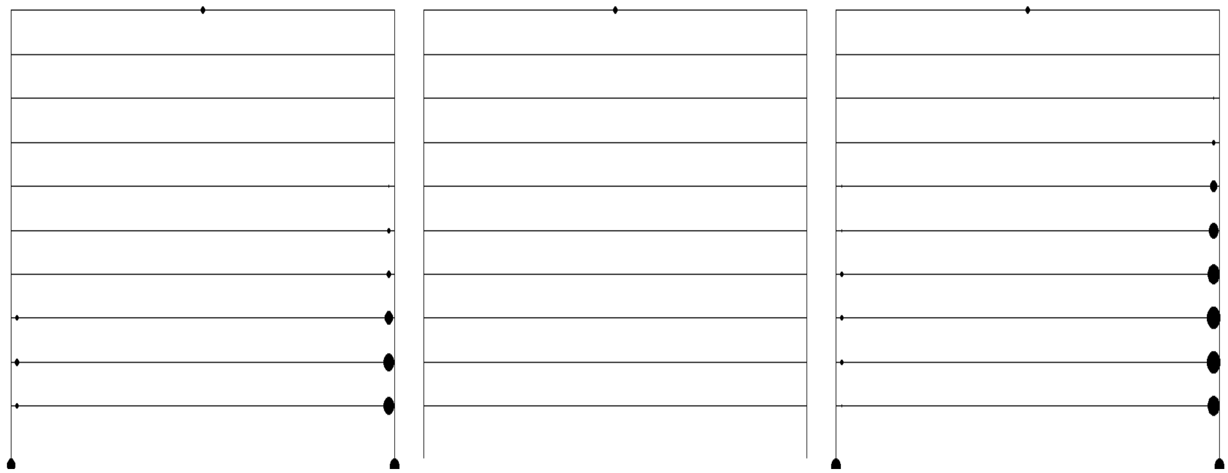

a) $+H_{EW}$ b) -V c) $+H_{EW}$-V

i) Inelastic behavior in dynamic analysis with the vertical ground motion from VCPS870207 record (case B)

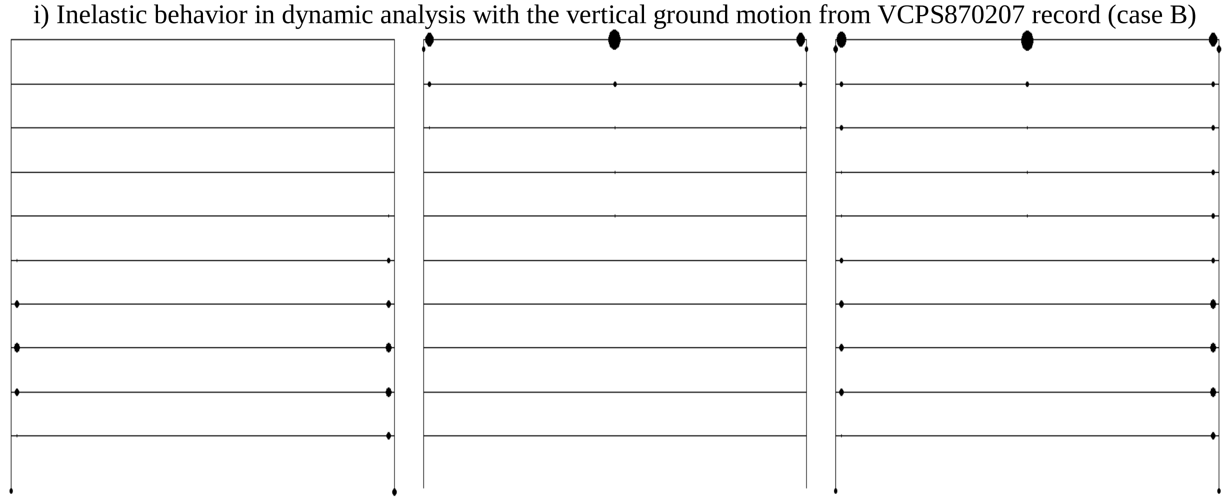

a) $+H_{NS}$ b) +V c) $+H_{NS}$+V

ii) Inelastic behavior in dynamic analysis with the vertical ground motion from VICS800609 record (case B)

Figure 7. Distribution of plastic hinge rotations on 10S1B model

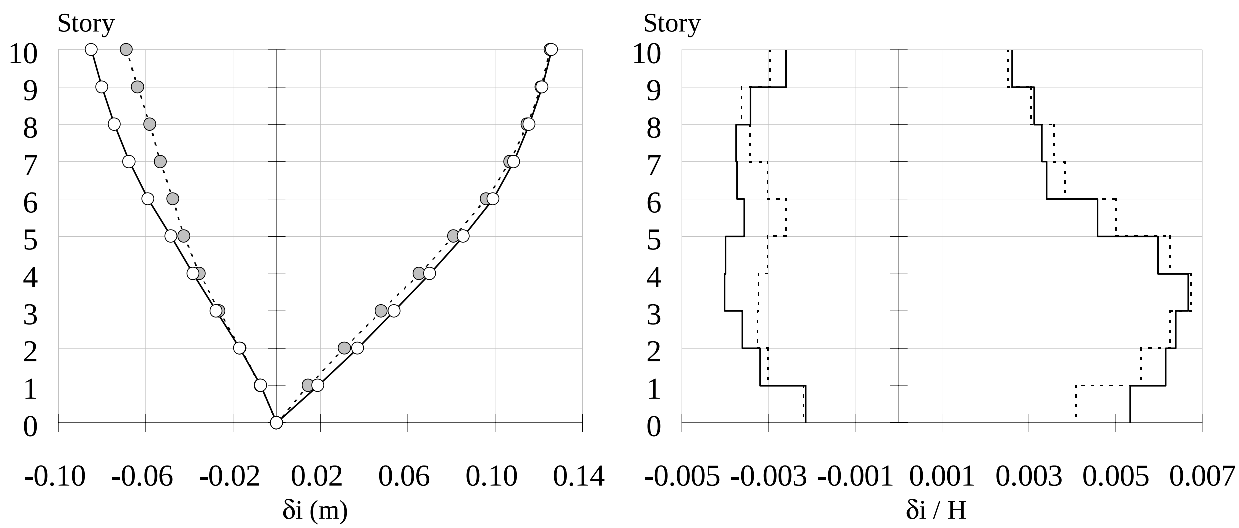

Figure 8. Maximum displacement and drifts for both unidirectional analysis (H, continuous line) and bi-directional analysis (H+V, dotted line) in model 10S1B, from record VICS800609 (case B).

In moment resistant frames with elastic-perfectly-plastic behavior, plastic hinge rotations occurred at both central and end sections of some beams, and at the ends of some columns. For those frames with significant dynamic amplification effects, the following trends were observed.

- Plastic hinge rotations at the center and ends of beams tend to increase with the period of the structural member in the vertical direction; the most unfavorable conditions are observed at the roof level beams, because of their less favorable restraint conditions. At the mid-span, plastic hinge rotations are generated by an increase in positive bending moments; the rotations at the ends of beams are associated with an increase in the negative bending moment. An inversion in the signs of the bending moments did not occur, and therefore, inverted plastic rotation in beams did not either. Thus, it seems that the minimum reinforcement ratios specified in codes for negative moment at mid-span and for positive moment at the ends is sufficient; nevertheless, it is may not be enough to provide ductility at such sections working as compression steel.

- Plastic hinge rotations in columns tend to be higher at the connections with long period beams, which generally correspond to the roof beams, because of their more unfavorable restraint conditions. As for the latter, the trend in the top floor columns is an increase in bending demand (up to 30%) while in the bottom ones the increase is for axial load demand (up to 60%). The case of the increase in bending demands implies an increase in the plastic hinge rotations, while the increase in the axial load implies a decrease in the rotation capacity; both effects tend to produce a failure mechanism in the columns by crushing of the concrete, which will be more serious if the transverse reinforcement is not enough. We suggest performing further research in order to evaluate the effects of both stiffness and resistance degradation in the elements.

The distribution of plastic hinge rotations considering the two components acting simultaneously is similar that which would be obtained from superposing the distributions that would occur independently, except in those cases where the same section has yielded with both acceleration histories. In those cases, variations on the structural behavior may exist in both directions; this is, impacting negatively in some events and impacting positively in others.

The increase in the damage on moment resistant frames produced by incorporation of the vertical component in the analysis is explained by the inertial forces that are generated in this direction, which produce increase and decrease in responses. The inertial forces on the beams have a direct influence on their supports, the columns, where the bending-compression response is directly affected.

The need to account for the influence of the vertical ground motion component on the dynamic response of beams may lead to an increase in their bending capacity. However, in order to avoid an undesirable plastic failure mechanism, the moment resistance of columns must be greater than that of the beams connected to them, in order to ensure a “strong column - weak beam” mechanism. The mentioned design requirement would not only be intended to avoid an undesirable failure mechanism, but also to account for the uncertainties about the bending-compression demands induced by the vertical component of strong ground motions.

CONCLUSIONS

The influence of the vertical seismic component on the non-linear dynamic response of some reinforced concrete structures was studied. For the dynamic step-by-step analyses were considered a set of ground motion records linked to earthquakes originated in the subduction zone of the Mexican Pacific Coast.

Additionally, general equations in order to estimate the fundamental vertical period for beams were also exposed in the paper. Particularly, an equation for beams connected to columns (frames) was proposed. This equation is function of the elastic stiffness in bending, the uniform load, the beam-span, and the non-dimensional parameter. The last parameter depends on the EI beam to column ratio, and it is perfectly consistent with its limit conditions.

For beams with the discussed common support conditions that have the same period and spectral demands in acceleration and displacement, similar rotation values were obtained. The latter indicates that the expected damage level for these beams is function of the earthquake intensity associated with the vertical period. This fact contradicts some recommended provisions because, according to them, just some elements (i.e. cantilever, prestressed and/or long-span beams), are vulnerable to vertical ground motions.

Based on both Mexican ground motion records and dynamic step-by-step analyses for the reinforced concrete moment resistant frames under study, the following behavior was observed:

A. If the system remains elastic under the combined action of gravitational loads and the vertical seismic component, both global and local responses are practically identical when: (1) the horizontal component acts alone and (2) when the horizontal and vertical components act simultaneously.

B. If the system reaches the non-linear behavior under the combined action of gravitational loads and the vertical seismic component, both global and local responses are notably different when (1) the horizontal component acts alone and (2) when the horizontal and vertical components act simultaneously.

It is not common to observe inelastic behavior in dynamic analyses considering exclusively the action of the vertical seismic component. Generally, ground motion records with a high vertical intensity are associated with shallow near-source earthquakes; these records frequently have high energy content in high frequencies. Because of this, large vertical dynamic responses are associated with systems with low vertical period; in this case, the displacement is small and so is the probability of occurrence of plastic hinge rotations. In cases with long vertical periods, spectral displacements are greater, but spectral accelerations are usually smaller and, consequently, the probabilities of plastic hinge rotations are low.

However, it was found that some vertical ground motion records corresponding to shallow earthquakes, (with both short epicentral distance and focal depth), lead some structural elements to yield even when acting alone, therefore, impacting negatively the structural behavior.

According to previous results, peak plastic hinge rotations occurred with the most intensive vertical records, this is, those with greater spectral pseudo-acceleration associated to the fundamental vertical period. All these records are associated to shallow-depth earthquakes and stations located near the epicenter, i.e., the Mexicali Valley records. The characteristics of these records are quite similar to those recorded in California (U.S.). Therefore, from the authors’ viewpoint, Californian records should be studied in order to verify if they adversely affect the seismic behavior of structures when the action of the vertical component is considered in the dynamic analyses.

Finally, it is concluded that additional studies are necessary in order to propose quantitative codified seismic design provisions applicable to sites where the vertical seismic component is important.

REFERENCES

1. Papazoglou, A. J. & Elnashai A. S. “Analytical and field evidence of the damaging effect of vertical earthquake ground motion”. Earthquake Engineering and Structural Dynamics. No. 25. 1996: 1109-1137.

2. Elnashai, A.S. “Seismic design with vertical earthquake motion”. Seismic Design Methodologies for the Next Generation of Codes. Balkerna, Rotterdam. 1997: 91-100.

3. Tani, S. & Soda, S. “Dynamics of reinforced concrete frames subjected to horizontal and vertical ground motions”. VII WCEE. Istanbul, Turkey. 1980.

4. Perea, T. “Introducción al estudio de la componente vertical de movimientos sísmicos y su influencia en el comportamiento estructural” (in Spanish). Master Thesis. DEPFI-UNAM. Mexico City. 2002.

5. Young, W. C. & Budynas, R. G. “Roark’s formulas for stress and strain”. Mc. Graw Hill. 7th. Edition. 2002.

6. Chopra, A. K. “Dynamics of structures: theory and applications to earthquake engineering”. Prentice Hall. USA. 1995.

7. Huang, T. C. “Eigenvalues and modifying quotients of vibration of beams, and eigenfunctions of vibration of beams”. Univ. Wis. Eng. Exp. Sta. Repts. 1964: 25-26.

8. Prakash, V. Powell, G. H. & Campbell S. “Drian-2DX. Base program description and user guide. Version 1.10”. Department of civil engineering. University of California. Berkeley, Ca., USA. 1993.

9. Powell, G. H. “Drian-2DX. Element description and user guide for element type01, type02, type04, type06, type09, and type15. Version 1.10”. Department of civil engineering. University of California. Berkeley, Ca., USA. 1993.

10. Sovero, G. "Un criterio de reducción por ductilidad del componente sísmico vertical" (in Spanish). P.h. Thesis. DEPFI-UNAM. Mexico City. 1986.